Priority Access and General Authorised Access Interference Mitigation in Spectrum Access System

Ying He, *Student Member, IEEE,* Beeshanga Abewardana Jayawickrama, *Member, IEEE,*
Eryk Dutkiewicz, *Member, IEEE,* Srikathyayani Srikanteswara, *Member, IEEE,*
and Markus Mueck, *Member, IEEE*

***Abstract*—To meet the capacity needs of next generation wireless communications, U.S. Federal Communications Commission has recently introduced Spectrum Access System. Spectrum is shared between three tiers - Incumbents, Priority Access Licensees (PAL) and General Authorised Access (GAA) Licensees. When the incumbents are absent, PAL and GAA share the spectrum under the constraint that GAA ensure the interference to PAL is no more than -40 dBm with at least 99% confidence. We consider the scenario where locations are not shared between PAL and GAA. We propose a PAL-GAA co-channel interference mitigation technique that does not expose base station locations. Our approach relies on GAA sharing the distribution and maximum number of transmitters in a finite area. We show how PAL can derive the distribution of the aggregated interference using Probability Density Function and Characteristic Function, and notify GAA about the exclusion zones in space that will guarantee that the interference requirement is met. We also propose a numerical approximation using Inverse Fast Fourier and Discrete Fourier Transforms. Analytically calculated distribution aligns well with the numerical results. Additionally we formulate an optimization problem for the optimal exclusion zone size. We analytically prove convexity of the problem. Our approach reduces the exclusion zone size by over 16%, which gives significantly more spectral opportunities to GAA in the spatial domain.**

***Index Terms*—Radio Spectrum Management, Spectrum Access System, Priority Access Licensees, General Authorised Access Licensees, Aggregated Interference.**

I. Introduction

A. Background

In the past few decades, many technologies have been developed and contributed to achieving high capacity in wireless networks. While we are seeking higher diversity in time, frequency, space and code domains, limited spectrum resource has remained a constraint. On our way to the next generation wireless communication [1], i.e. 5G, new approaches for effective utilization of limited spectrum have been proposed to break the physical constraint and to help to reach the goal of 5G: 1000 times higher capacity [2].

Recently, regulatory bodies have been promoting spectrum sharing to facilitate this capacity growth. Two prominent spectrum sharing schemes are 1) Licensed Shared Access (LSA) and 2) Spectrum Access System (SAS). LSA is being developed by ETSI in Europe for the 2.3-3.4 GHz band [3]. SAS focuses on the 3.55-3.7 GHz band in US, and it is being developed by FCC [4] and [5]. Both schemes open up access to previously restricted mobile communications bands below 6 GHz. [6] gives an comprehensive and comparative overview of LSA and SAS. [7] provides a review on different interest groups' viewpoint on FCC proposed SAS architecture. The WInnF Spectrum Sharing Committee (SSC) of the Wireless Innovation Forum (WInnF) has released several reports recently about SAS [8], [9], [10] and [11]. Several leading industrial companies contributed to the forum to push the development for SAS.

LSA proposed a two-tier sharing architecture between incumbents and licensees. MNOs get access to licensed spectrum when incumbents are absent at the time or the same geolocation area. There will be no co-channel interference between incumbents and licensees. In contrast, SAS proposed a three-tier sharing model. Incumbent users represent the highest tier in the framework and receive interference protection from Citizens Broadband Radio Service users. The Citizens Broadband Radio Service itself consists of two tiers - Priority Access and General Authorized Access (GAA) both authorized in any given location and frequency by an SAS. PAL/GAA licenses are issued by SAS for a finite census tract as shown in Fig. 1. A census tract is defined as a statistical subdivision of a county or equivalent entity. PAL, defined as an authorization to use a 10 MHz channel in a single census tract for three years, will be assigned in up to 70 MHz of the 3.55 - 3.7 GHz portion of the band. GAA is allowed to use throughout 150 Mhz. Priority Access operations receive protection from GAA operations.

The PAL-GAA interference requirement is defined in Section 96.41 (f) of [4] as follows:

"*Priority Access Licensees must accept adjacent channel and in-band blocking interference (emissions from other authorized Priority Access or GAA CBSDs transmitting between 3550 and 3700 MHz) up to a power spectral density level not to exceed -40 dBm in any direction with greater than 99% probability when integrated over a 10 megahertz reference bandwidth, with the measurement antenna placed at a height of 1.5 meters above ground level, unless the affected Priority Access Licensees agree to an alternative limit and communicates that to the SAS.*"

We consider co-channel interference as the main contributor to the aggregated interference. We assume the adjacent channel

Y. He, B. A. Jayawickrama and E. Dutkiewicz are with University of Technology Sydney, Global Big Data Technology Centre (e-mail: ying.he-6@student.uts.edu.au; beeshanga.jayawickrama@uts.edu.au; eryk.dutkiewicz@uts.edu.au). S. Srikanteswara is with Intel Corporation, Portland, U.S. (e-mail: srikathyayani.srikanteswara@intel.com). M. Mueck is with Intel Mobile Communications, Munich, Germany (e-mail: markus.dominik.mueck@intel.com).

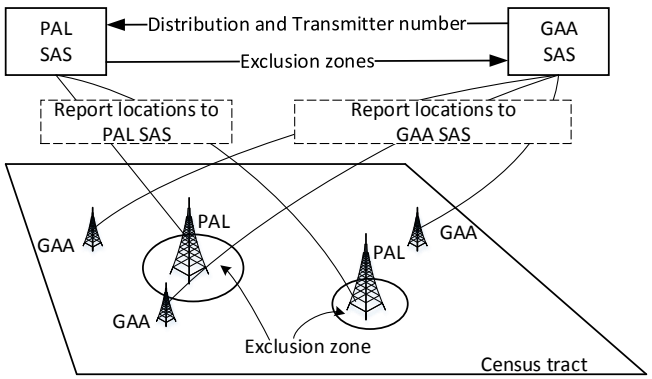

Fig. 1. Illustration of inter-SAS interference mitigation, PAL base stations are connected to PAL SAS and GAA base stations are connected to GAA SAS.

interference can be neglected. There can be multiple GAA transmitters and multiple PAL receivers in the same census tract. One possible way to control the interference is that the PAL network estimates the aggregated interference using the location information of the GAA transmitters. The interference can be controlled below a certain threshold by adjusting the transmit power of each GAA with either a binary decision or an optimised power level. The Radio Environment Maps [12] method can be used in such a scenario. However, this method is only applicable when the PAL/GAA network has precise information about the locations of the other network's base stations.

In a practical scenario, if the GAA transmitters and the PAL receivers belong to the same operator, the location information is known to all, since each PAL/GAA is obliged to regularly inform about its location to the corresponding SAS [4]. However, if the GAA transmitters and the PAL receivers belong to different operators, the location information is not necessarily known. The locations of the base stations are regarded as private information by operators. The operators in U.S. have taken a strong stance against sharing the site locations with all SAS users (including competitors) to a degree that they would opt out from using SAS if that was an obligation. One option would be for PAL to conservatively assign a large exclusion zone outside which GAA can be located anywhere, such that the interference constraints are met. However such a worst case approach will result in a large decrease in the spectral chances of GAA network in the spatial domain. Therefore, the motivation of this paper is to develop a generic framework to find the smallest possible exclusion zones that guarantee interference protection to PAL, without exchanging the location information.

B. Related Work

Several previous studies on cognitive radio networks regarding aggregated interference are related to this topic. Some studies assumed Poisson Point Process (PPP) as the distribution of the users. [13] studied the aggregated interference from secondary users to a primary user by deriving the Moment Generating Function (MGF) and cumulants in a finite disk area. [14] studied the aggregated interference from secondary users to primary users in cognitive radio networks with exclusion zones around primary users and proposed approximations based on the Poisson cluster process. [15] analyzed the aggregated interference in an underlay network of cognitive radio with Rayleigh fading and exponential path loss. [16] derived the results of the higher order moments of the Signal-to-Interference-plus-Noise Ratio (SINR) using the MGF and showed the existence of a tradeoff between the average SINR and rate performance in cellular networks. Some other studies assumed uniform distribution for the users. [17] considered that an independent and uniform distribution is more suitable for the cognitive radio network scenario and proposed to use a finite arbitrarily-shaped model for the network. [17] also introduced a numerical approximation of the Laplace transformation to perform the MGF. [18] studied secondary user activity protocols' effects on the performance of underlay cognitive radio networks. Both [17] and [18] are based on the distance distribution calculation in a finite area proposed in [19].

In the SAS scenario, a census tract is a closed area with possibly an irregular shape. The performance, such as network capacity, should depend on the physical boundary of the census tract. Thus we believe a finite arbitrarily-shaped model is more suitable for a census tract than a disk. Moreover, we adopt the assumption in [17] that the location of users follow an independent and uniform distribution. All the above papers used the MGF to derive the distribution of aggregate interference from the distribution of the interference from a single user. The Laplace transform used to perform the MGF has high computational complexity and it is difficult to implement. Furthermore, the previous related studies focused on one receiver scenario. However, in the SAS framework, there will be multiple PAL base stations in a census tract and we need to keep interference at all of them below the threshold.

A few recent studies are also related regarding using exclusion zones to protect primary users (i.e. incumbents) from secondary users (i.e. LSA/SAS licensees). Several methods are based on measurement and monitoring of interference. [20] provides the assumptions, methods and analyses of how to design exclusion zones in the 3.5 GHz band. [21] mentioned dynamically monitoring the activity of incumbents and inform secondary users. Other methods are based on distribution features of interference. [22] studied the optimal deployment of secondary users. [23] proposed and compared three exclusion zone designs and Media Access Control (MAC) protocol accordingly. [24] studied interference from secondary users to incumbents in SAS. [24] proposed a multi-tier exclusion zone design to improve the spectrum efficiency. [25] proposed a dynamic exclusion zone design in SAS to protect the incumbents from secondary users by dividing a disk area into several annular sectors and provided aggregated interference distribution with a Normal approximation. Both [24] and [25] used annular sectors with the incumbent at the center. The practical network deployment area is difficult to model with annular sectors, since it can be any possible shaped finite area. Moreover, we can directly calculate the Probability Density Function (PDF) of the aggregated interference instead of using an approximation.

In summary, there is so far no suitable solution for the aggregated interference mitigation between PAL (i.e. second-tier) and GAA (i.e. third-tier) in SAS.

C. Contribution

In this paper, we propose a method to mitigate SAS PAL GAA co-channel aggregated interference in one census tract without exposing the geo-locations. We make the following contributions:

- To the best of our knowledge, our method is the first SAS PAL GAA co-channel aggregated interference mitigation without exposing the locations of any SAS networks.
- The information shared between GAA and PAL is not adequate for any network to derive or estimate the others' locations. Thus the information security is guaranteed.
- Given a certain GAA distribution and maximum transmitter number parameter setting, there are only two messages communicated between two SASs. There is less information sharing and a lower hand-shake overhead compared to measuring and feedback methods as discussed in Section I.
- Our method considers multiple PAL interference receivers and the effects of the changes of the other exclusion zones on the interference.
- We derive an aggregated interference distribution with overlapping exclusion zones.
- PAL location can be different from the geometric center of the exclusion zone that is more applicable for practical scenarios.
- We propose to use a Characteristic Function (CF) instead of a MGF to obtain the multiple-transmitter aggregated interference distribution from the single-transmitter interference distribution. Furthermore, we introduce the widely used Inverse Fast Fourier Transform (IFFT) and Discrete Fourier Transform (DFT) as the numerical solution for future practical implementation of our method.
- We optimize the exclusion zone size targeting at minimum exclusion zone area to keep the fairness between PAL and GAA base stations.
- We propose a lower bound for the constraints of the optimization problem to turn it from a non-convex problem into a convex problem.
- Our approach reduces the exclusion zone size by over 16%, which gives significantly more spectral opportunities to GAA in the spatial domain.

D. Organization

The rest of this paper is organized as follows: Section II introduces the system model. We derive the distribution of the distance from GAA base stations to PAL base stations in Section III and the distribution of the aggregated interference in Section IV. A numerical approximation is given in Section V. We present the optimization problem in Section VI. Simulation results are shown in Section VII and conclusions are given in Section VIII.

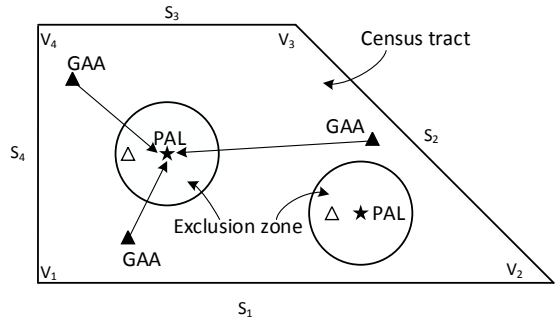

Fig. 2. SAS PAL GAA co-channel interference illustration:★ are the PAL base stations, ▲ are the GAA base stations outside of exclusion zones that can transmit, △ are the GAA base stations inside of exclusion zones that have to keep silent. $V_i, i = 1, ..., 4$ are the vertices, $S_i, i = 1, ..., 4$ are the sides.

II. System Model

We consider the scenario, illustrated in Fig. 2: one operator owns the census tract and it is running PAL. The other operator runs GAA in the same census tract using the same spectrum. We model the census tract as a closed polygon shaped area. Assume the PAL and GAA are all the base stations with fixed locations and GAA base stations are transmitting with a known power. We define PAL base stations as interference receivers and GAA base stations as interference transmitters in this paper. As interference receivers, the PAL network has full knowledge of all base stations of it own network. We assume that the small scale fading can be averaged out. Shadow fading or height differences of antennas are not considered in this paper. We use the exclusion zone concept [3] to control the interference to the PAL base stations and mask their locations. Any GAA transmission inside of the exclusion zone can not transmit. We use each PAL base station j as the center and draw a circle with a certain radius around it to form the exclusion zone. If two exclusion zones overlap, we group them into one combined exclusion zone with their non-overlapping boundary, each PAL base station is still at the center of its previous exclusion zone circle. If more than two exclusion zones overlap, we use one circle to replace their exclusion zones with the minimum area that covers all overlapping exclusion zones, while the PAL base stations may no longer be at the center of the new circle.

For each PAL interference receiver j, the constraint on aggregated interference I_j is formulated as:

$$P(I_j \leq I_0) > P_0 \tag{1}$$

In the default case, $I_0 = -40$ dBm, $P_0 = 0.99$. The aggregated interference at PAL receiver j from N_{TX} number of GAA transmitters is given as:

$$I_j = \sum_{i=1}^{N_{TX}} I_{ij} \tag{2}$$

i is the index of the interference transmitters, i.e. GAA, $i \in \{1, ..., N_{TX}\}$. The interference from each transmitter i is given as:

$$I_{ij} = P_t L_{ij} \tag{3}$$

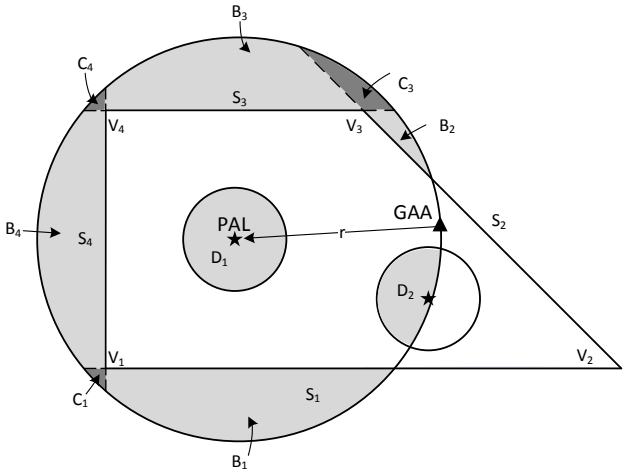

Fig. 3. Illustration of CDF of the distance of GAA interference transmitters to a PAL interference receiver, B_l is the area outside of the side S_l of the census tract, C_j is the overlapping area of B_l and B_j and D_k is the overlapping area of the exclusion zone k and the circle whose center is the PAL interference receiver's location and radius is r.

We use the path loss model in [26],

$$L_{ij} = K\left(\frac{d_0}{d_{ij}}\right)^{\beta} \tag{4}$$

where d_{ij} is the distance from interference transmitter i to receiver j.

We propose the process of the PAL-GAA co-channel interference mitigation as follows: The GAA network will initiate a request to the PAL network with the information of the distribution and the number of GAA transmitters. The PAL network will use the GAA information to obtain the PDF of the distance of one GAA transmitter to a PAL receiver, then use the transformation function to get the PDF of the interference from one GAA transmitter to a PAL receiver. The Characteristic Function is leveraged to calculate the PDF of the aggregated interference from multiple GAA transmitters to a PAL receiver. The CDF of the aggregated interference from multiple GAA transmitters to a PAL receiver is a integral of the PDF. A numerical approximation of the CDF is implemented by IDFT, multiplication and DFT. From the CDF, the probability of the aggregated interference below a certain threshold is obtained. The PAL network then can optimize the exclusion zones around all PAL receivers and send the exclusion zone information back to the GAA network. After the GAA network receives feedback from the PAL network on the exclusion zones, it will launch the GAA transmission accordingly. This is one round of the PAL-GAA interference mitigation. If any parameter in the GAA transmission changes, the GAA network will send a new request to the PAL network and that will trigger a new round of interference mitigation. The key components in the process are presented in detail in the following sections.

III. Distribution of distance of a GAA transmitter to a PAL receiver

Since we assume the interference transmitters' locations follow a uniform distribution inside of the finite census tract excluding the exclusion zone of each receiver, the distribution of the distance from the transmitter to a particular receiver can be derived [17]. In [17], the Cumulative Density Function (CDF) of the distance r from a transmitter to a certain receiver is defined as:

$$F_R(r) = \frac{1}{|A|}\left(\pi r^2 - \sum_l B_l + \sum_l C_l\right) \tag{5}$$

The difference is that we consider that GAA interference transmitters have to keep silent in other exclusion zones. Thus in this paper, the CDF of the distance r from a transmitter to a certain receiver is given as:

$$F_R(r) = \frac{1}{|A^c| - \sum_{k=1}^{N_E}\left|A_k^e\right|}\left(\pi r^2 - \sum_l B_l + \sum_l C_l - \sum_{k=1}^{N_E} D_k(r)\right) \tag{6}$$

where $|A^c|$ is the area of the census tract, $\left|A_k^e\right|$ is the area of the exclusion zone k, and N_E is the total number of exclusion zones. One exclusion zone may contain more than one PAL base station, thus $N_E \leq N_{RX}$, N_{RX} is the number of PAL base stations. $B_l(r)$ and $C_l(r)$ depend on the location of PAL j and the shape of the census tract, shown in Fig. 3 and given as follows:

$$B_l(r) = 2\int_{d_l}^{r} \tau \arccos\left(\frac{d_l}{\tau}\right) d\tau \tag{7}$$

$$C_l(r) = \int_{d_l}^{r}\left(\tau\left(-\pi + \delta_l + \arccos\left(\frac{d_l}{\tau}\right) + \arccos\left(\frac{d_{l-1}}{\tau}\right)\right)\right) d\tau \tag{8}$$

where δ_l is the inner angle of vertex l.

$D_k(r)$ shown in Fig. 3, varies with the exclusion zone and the number of PAL base stations inside of exclusion zone k. We divide this into two cases: calculate $D_k(r)$ with regard of its own exclusion zone with PAL base station j inside and with regard of the other exclusion zones.

A. Calculation of $D_k(r)$ for exclusion zone k that covers PAL receiver j

If only one PAL base station j is inside of its own exclusion zone, PAL base station j is at the center of the exclusion zone circle, $D_k(r) = 0$ when $r <= R_k$ and $D_k(r) = \left|A_k^e\right|$ when $r > R_k$.

If two PAL base stations are inside of its own exclusion zone of two combined circles with radius R_{k_1} and R_{k_2}, we assume R_{k_1} is the radius of the circle with PAL base station j as the center.

$$D_k(r) = 2\int_{r_{min}}^{r} \tau\xi_{jk_2}(\tau)d\tau \tag{9}$$

where

$$\xi_{jk_i}(r) = \arccos\left(\frac{r^2 + d_{jk_i}^2 - R_{k_i}^2}{2d_{jk_i}r}\right) \tag{10}$$

and $r_{min} = R_{k_1}$. d_{jk_2} is the distance between PAL base station j to the other PAL base station k_2 in the same exclusion zone. $\tau = r'$.

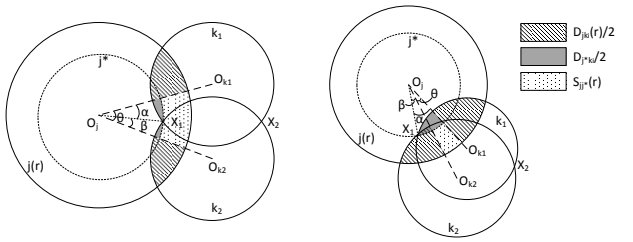

(a) (b)

Fig. 4. Illustration for two overlapping exclusion zone. When $\min\left(d_{jk}^X\right) < r < \max\left(d_{jk}^X\right)$, only one intersection point X_1 is covered by circle $j(r)$. (a): $c_1 = 1, \theta = \alpha + \beta$; (b):$c_1 = -1, \theta < \alpha + \beta$. Note: $D_{j^*k_2}$ area is overlapping with $D_{jk_2}(r)$ and D_{j^*k1} in (b).

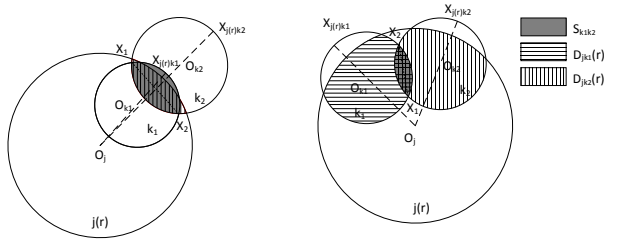

(a) (b)

Fig. 5. Illustration for two overlapping exclusion zones. $\max\left(d_{jk}^X\right) \le r < \max\left(d_{jk_i}\right) + R_k$, both intersection points X_1 and X_2 are covered by circle $j(r)$. (a): $c_2 = 0$ $X_{j(r)k1}$ and $X_{j(r)k2}$ are on the same side of the line X_1,X_2; (b): $c_2 = 0$ $X_{j(r)k1}$ and $X_{j(r)k2}$ are on different sides of the line X_1,X_2. Note: $S_{k_1k_2}$ is overlapping with $D_{jk_2}(r)$ in (a); $S_{k_1k_2}$ is overlapping with $D_{jk_1}(r)$ and $D_{jk_2}(r)$ in (b).

If more than two PAL base stations are inside of its own exclusion zone k,

$$D_k(r) = 2\int_{r_{min}}^{r} \tau\xi_{jk}(\tau)d\tau \tag{11}$$

where $\xi_{jk}(r)$ follows (10), r_{min} is the minimum distance from PAL base station j to the boundary of exclusion zone k, d_{jk} is the distance between PAL base station j to the geometric center of exclusion zone k.

B. Calculation of $D_k(r)$ for the exclusion zone k that does not cover the PAL receiver j

If there is only one PAL base station in another exclusion zone k that does not cover PAL base station j,

$$D_k(r) = 2\int_{r_{min}}^{r} \tau\xi_{jk}(\tau)d\tau \tag{12}$$

where $r_{min} = d_{jk} - R_k$, d_{jk} is the distance between PAL base station j to the other PAL base station k.

If there are two PAL base stations in another exclusion zone k, we derive $D_k(r)$ as follows:

When two PAL exclusion zones are overlapping, we combine them into one exclusion zone k and denote the two individual PAL exclusion zones as k_1 and k_2. We define: 1) the locations of two PAL base stations which are the centers of exclusion zone k_1 and k_2 as O_{k1} and O_{k2} respectively; 2) the intersection points of k_1 and k_2 as X_1 and X_2; 3) the circle with PAL base station j as the center and distance r as the radius of circle $j(r)$; 4) location of PAL base station j as O_j and 5) the distance from O_j to X_1 and X_2 as set d_{jk}^X. We then calculate the intersection area $D_k(r)$ between circle $j(r)$ and exclusion zone k.

We divide this problem into three different cases according to the range of distance r:

1) $\min\left(d_{jk_i}\right) - R_k < r \le \min\left(d_{jk}^X\right)$, neither X_1 or X_2 is covered by circle $j(r)$
   If the circle overlapping with $j(r)$ is k_1, k_2 or both, the intersection area is equal to the summation of the intersection area with an individual exclusion zone. $D_k(r) = D_{jk_1}(r) + D_{jk_2}(r)$, where $D_{jk_i}(r)$ follows (12).
2) $\min\left(d_{jk}^X\right) < r < \max\left(d_{jk}^X\right)$, only one of X_1 or X_2 is inside of circle $j(r)$
   As shown in Fig. 4, we assume X_1 is inside of circle $j(r)$. We define the condition c_1 as:

$$c_1 = \begin{cases} 1 & \theta = \alpha + \beta \\ -1 & \theta < \alpha + \beta \end{cases} \tag{13}$$

   where

$$\theta = O_{k_1}\hat{O}_j O_{k_2} \tag{14}$$

$$\alpha = O_{k_1}\hat{O}_j O_{X_1} \tag{15}$$

$$\beta = O_{k_2}\hat{O}_j O_{X_1} \tag{16}$$

   a) $c_1 = 1$
   The overlapping area of $j(r)$ and exclusion zone k in Fig. 4 (a) is given as

$$D_k(r) = \frac{D_{jk_1}(r)}{2} + \frac{D_{jk_2}(r)}{2} + \frac{D_{j^*k_1}}{2} + \frac{D_{j^*k_2}}{2} + S_{j^*j}(r) \tag{17}$$

   b) $c_1 = -1$
   The overlapping area of A and exclusion zone k in Fig. 4 (b) is given as

$$D_k(r) = \frac{D_{jk_1}(r)}{2} + \frac{D_{jk_2}(r)}{2} + \frac{D_{j^*k_1}}{2} - \frac{D_{j^*k_2}}{2} + S_{j^*j}(r) \tag{18}$$

   where $D_{jk_1}(r)$ and $D_{jk_2}(r)$ are the intersection areas of circle j and circles k_1 and k_2 respectively, following (12). $D_{j^*k_1}$ and $D_{j^*k_2}$ are the intersection areas of circle j^* and circles k_1 and k_2 respectively. Circle j^* is the concentric circle with circle $j(r)$ and radius R_{j^*} which is the distance from O_j to X_1. $S_{j^*j}(r)$ is the area between circle j^* and circle $j(r)$ with the angle θ. $S_{j^*j}(r) = (r^2 - R_{j^*}^2)\theta$. $D_{j^*k_1}$, $D_{j^*k_2}$ and θ are constant to the change of r. The derivative of (17) and (18) is the same as

$$\frac{\partial D_k(r)}{\partial r} = r\xi_{jk_1}(r) + r\xi_{jk_2}(r) + 2r\theta \tag{19}$$

   where $\xi_{jk_i}(r)$ follows (10).
3) $\max\left(d_{jk}^X\right) \le r < \max\left(d_{jk_i}\right) + R_k$, both X_1 and X_2 are covered by circle $j(r)$

As shown in Fig. 5, we connect the centers of the two circles O_j and O_{k1} with a straight line and extend it to get the intersection point $X_{j(r)k1}$ at the exclusion zone k_1. Likewise, we can get the intersection point $X_{j(r)k2}$. We connect X_1 and X_2 with a straight line and define the function of the line as $g(\bullet) = 0$, $\bullet$ denotes the coordinates of the points on the line. We define the condition c_2 as

$$c_2 = \begin{cases} 0 & \text{sign}\left(g\left(X_{j(r)k1}\right)\right) = \text{sign}\left(g\left(X_{j(r)k2}\right)\right) \\ 1 & \text{sign}\left(g\left(X_{j(r)k1}\right)\right) \neq \text{sign}\left(g\left(X_{j(r)k2}\right)\right) \end{cases} \tag{20}$$

which gives $c_2 = 0$ if $X_{j(r)k1}$ and $X_{j(r)k2}$ are on the same side of the line $g(\bullet) = 0$ and $c_2 = 1$ if $X_{j(r)k1}$ and $X_{j(r)k2}$ are on different sides of the line $g(\bullet) = 0$.

a) $c_2 = 0$
As shown in Fig. 5 (a), the overlapping area of circle $j(r)$ and exclusion zone k is given as

$$D_k(r) = |A_{k_1}| - S_{k_1k_2} + D_{jk_2}(r) \tag{21}$$

where $|A_{k_1}|$ is the area of exclusion zone k_1, $S_{k_1k_2}$ is defined as the intersection area of exclusion zone k_1 and k_2. $D_{jk_2}(r)$ is defined as the intersection area of circle $j(r)$ and exclusion zone k_2. $|A_{k_1}|$ and $S_{k_1k_2}$ are constant to the change of r. The derivative of (21) is

$$\frac{\partial D_k(r)}{\partial r} = 2r\xi_{jk_2}(r) \tag{22}$$

where $\xi_{jk_i}(r)$ follows (10).

b) $c_2 = 1$
As shown in Fig. 5 (b), the overlapping area of circle $j(r)$ and exclusion zone k is given as

$$D_k(r) = D_{jk_1}(r) + D_{jk_2}(r) - S_{k_1k_2} \tag{23}$$

where $D_{jk_1}(r)$ is defined as the intersection area of circle $j(r)$ and exclusion zone k_1 and $D_{jk_2}(r)$ is defined as the intersection area of circle $j(r)$ and exclusion zone k_2. The derivative of (23) is

$$\frac{\partial D_k(r)}{\partial r} = 2r\xi_{jk_1}(r) + 2r\xi_{jk_2}(r) \tag{24}$$

where $\xi_{jk_i}(r)$ follows (10).

In summary, when two PAL base stations are inside of exclusion zone k, $D_k(r)$ is given as (25), where $D_{jk_i}(r)$ is the intersection area of circle j and circle k_i. d_{jk}^X is the set of the distance from the center of circle j to two intersection points X_1 and X_2 of the exclusion zone k. $\frac{\partial D_k(r)}{\partial r}$ is given as (26), where $\xi_{jk_i}(r)$ follows (10).

If more than two PAL base stations are inside of exclusion zone k,

$$D_k(r) = 2\int_{r_{min}}^{r} \tau\xi_{jk}(r)d\tau \tag{27}$$

where $\xi_{jk}(r)$ follows (10), $r_{min} = d_{jk} - R_k$, d_{jk} is the distance between PAL base station j to the geometric center of exclusion zone k.

Deriving (6), the PDF of distance r is given as

$$f_R(r) = \frac{2\pi r - \sum_l \frac{\partial B_l}{\partial r} + \sum_l \frac{\partial C_l}{\partial r} - \sum_{k=1}^{N_E} \frac{\partial D_k}{\partial r}}{|A^c| - \sum_{k=1}^{N_E} \left|A_k^e\right|} \tag{28}$$

where

$$\frac{\partial B_l(r)}{\partial r} = 2r\arccos\left(\frac{d_l}{r}\right) \tag{29}$$

$$\frac{\partial C_l(r)}{\partial r} = r\left(-\pi + \delta_l + \arccos\left(\frac{d_l}{r}\right) + \arccos\left(\frac{d_{l-1}}{r}\right)\right) \tag{30}$$

When $D_k(r)$ follows (9), (11), (12) and (27),

$$\frac{\partial D_k(r)}{\partial r} = 2r\arccos\left(\frac{r^2 + d_{jk}^2 - R_k^2}{2d_{jk}r}\right) = 2r\xi_{jk}(r) \tag{31}$$

where d_{jk}, R_k and the feasible range of r follows the parameter settings in (9), (11), (12) and (27) respectively.

When $D_k(r)$ follows (25), $\frac{\partial D_k(r)}{\partial r}$ is given as (26), where $\xi_{jk_i}(r)$ follows (10).

IV. Distribution of aggregated interference from multiple GAA transmitters

We derive the PDF of interference from a transmitter to the receiver j using the transformation function in [27]

$$f_Y(y) = f_R\left(r(y)\right)\left|\frac{dr}{dy}\right| \tag{32}$$

where $r(y)$ is the inverse function of the path loss given as:

$$y(r) = P_t K\left(\frac{d_0}{r}\right)^{\beta} \tag{33}$$

Thus, we have

$$r(y) = (My)^{\lambda} \tag{34}$$

where $M = (d_0)^{-\beta}/(KP_t)$ and $\lambda = -1/\beta$. Thus the PDF of the interference is given as:

$$f_Y(y) = f_R\left((My)^{\lambda}\right)\left|\lambda M(My)^{\lambda-1}\right| \tag{35}$$

where y represents a random variable of individual interference from transmitter i to receiver j, I_{ij}.

We assume the transmitters are independent and uniformly distributed inside of the census tract. Therefore the interference from the transmitters follow the same and independent distribution. Thus the PDF of the aggregated interference can be derived as [28]:

$$f_Z(z) = \underbrace{f_Y(y) * f_Y(y) * \ldots * f_Y(y)}_{N_{TX}} \tag{36}$$

where z represents a random variable of aggregated interference from multiple transmitters to receiver j, I_j.

Convolution becomes complex and time consuming when the number of transmitters N_{TX} is large. Alternatively, we propose to use the Fourier Transform which is widely used in digital signal processing and communication systems. We use DFT to obtain a numerical approximation for future practical implementation.

$$D_k(r) = \begin{cases} D_{jk_1}(r) + D_{jk_2}(r) & \min\left(d_{jk_i}\right) - R_k < r \leq \min\left(d_{jk}^X\right) \\ \dfrac{D_{jk_1}(r)}{2} + \dfrac{D_{jk_2}(r)}{2} + \dfrac{D_{j^*k_1}}{2} + c_1\dfrac{D_{j^*k_2}}{2} + S_{j^*j}(r) & \min\left(d_{jk}^X\right) < r < \max\left(d_{jk}^X\right) \\ |A_{k_1}| - S_{k_1k_2} + D_{jk_2}(r) & \max\left(d_{jk}^X\right) \leq r < \max\left(d_{jk_i}\right) + R_k \text{ and } \overline{c_2} \\ D_{jk_1}(r) + D_{jk_2}(r) - S_{k_1k_2} & \max\left(d_{jk}^X\right) \leq r < \max\left(d_{jk_i}\right) + R_k \text{ and } c_2 \end{cases} \tag{25}$$

$$\frac{\partial D_k(r)}{\partial r} = \begin{cases} 2r\xi_{jk_1}(r) + 2r\xi_{jk_2}(r) & \min\left(d_{jk_i}\right) - R_k < r \leq \min\left(d_{jk}^X\right) \\ r\xi_{jk_1}(r) + r\xi_{jk_2}(r) + 2r\theta & \min\left(d_{jk}^X\right) < r < \max\left(d_{jk}^X\right) \\ c_2 \times 2r\xi_{jk_1}(r) + 2r\xi_{jk_2}(r) & \max\left(d_{jk}^X\right) \leq r < \max\left(d_{jk_i}\right) + R_k \end{cases} \tag{26}$$

The Characteristic Function (CF) of the aggregated interference is given as:

$$\Phi_Z(t) = \int e^{itz} f(z) dz \tag{37}$$

assign $t = 2\pi k$, (37) then becomes

$$\Phi_Z(2\pi k) = \int e^{i2\pi kz} f(z) dz = \mathcal{F}^{-1}\left[f_Z(z)\right] \tag{38}$$

According to the CF property, the CF of the aggregated interference is the multiplication of the CF of the individual interferences [29].

$$\begin{aligned} \Phi_Z(2\pi k) &= \prod_{i=1}^{N_{TX}} \Phi_Y(2\pi k) = \left(\Phi_Y(2\pi k)\right)^{N_{TX}} \\ &= \left(\int e^{i2\pi ky} f_Y(y) dy\right)^{N_{TX}} \end{aligned} \tag{39}$$

where $f_Y(y)$ is obtained from (35). According to (38) the PDF of the aggregated interference is given as:

$$\begin{aligned} f_Z(z) &= \mathcal{F}[\Phi_Z(2\pi k)] = \mathcal{F}\left[\left(\int e^{i2\pi ky} f_Y(y) dy\right)^{N_{TX}}\right] \\ &= \mathcal{F}\left[\left(\mathcal{F}^{-1}\left[f_Y(y)\right]\right)^{N_{TX}}\right] \end{aligned} \tag{40}$$

Thus we can calculate the CDF of the aggregated interference

$$F_Z(z) = \int_{-\infty}^{z} f_Z(t) dt = \int_{-\infty}^{z} \mathcal{F}\left[\left(\mathcal{F}^{-1}\left[f_Y(y)\right]\right)^{N_{TX}}\right] dt \tag{41}$$

We can calculate the probability of the aggregated interference to receiver j less or equal to I_0 by

$$P(I_j \leq I_0) = F_Z^j(I_0) \tag{42}$$

where $F_Z^j(I_0)$ follows (41).

V. Numerical Approximation

In general it is difficult to get a closed-form result for (41), thus we use DFT and Inverse Discrete Fourier Transform (IDFT) to approximate the Fourier transform in (41)

$$\begin{aligned} F_Z(z) &\approx \int_{-\infty}^{z} DFT\left[\left(IDFT\left[f_Y(y)\right]\right)^{N_{TX}}\right] dt \\ &= \int_{-\infty}^{z} \sum_{k=0}^{N_{\text{DFT}}-1} \left[\left(\sum_{n=0}^{N_{\text{IDFT}}-1} Y(n) e^{\frac{\mathrm{j}2\pi nk}{N_{\text{IDFT}}}}\right)^{N_{TX}}\right] dt \end{aligned} \tag{43}$$

where $Y(n)$ is a digital sample sequence of $f_Y(y)$ with zero padding, given as:

$$Y(n) = \begin{cases} f_Y(nT_s) & \text{for } n = 0, 1, \cdots, N_s - 1 \\ 0 & \text{for } m = N_s, \cdots, N_{\text{IDFT}} - 1 \end{cases} \tag{44}$$

where $N_{IDFT} = N_{TX} \times N_s$, N_s is the sample number and T_s is the sample interval. When the number of transmitters N_{TX} increases, the size of IDFT also increases, so does the computational complexity. We proposed to divide IDFT into groups of IFFTs to decrease the computational complexity [30]. We assume the value of N_s is a power of two. Let $n = aM + b$ where $M \triangleq N_{\text{IDFT}}/N_{\text{IFFT}}$ is the total number of groups, $a = 0, 1, \cdots, N_{\text{IFFT}} - 1$ is the data index in a group and $b = 0, 1, \cdots, M-1$ is the group index. The b-th group can be rewritten as $Y(n) = Y(aM + b)$, thus the IDFT is given as:

$$\begin{aligned} \sum_{n=0}^{N_{\text{IDFT}}-1} Y(n) e^{\frac{\mathrm{j}2\pi nk}{N_{\text{IDFT}}}} &= \sum_{m=0}^{N_{\text{IFFT}}-1} Y(aM+b) e^{\frac{\mathrm{j}2\pi am}{N_{\text{IFFT}}}} \\ &= \sum_{m=0}^{N_{\text{IFFT}}-1} \left[Y_1(m) \times Y_2(b,m)\right] e^{\frac{\mathrm{j}2\pi am}{N_{\text{IFFT}}}} \end{aligned} \tag{45}$$

where

$$Y_1(m) = \begin{cases} f_Y(mT_s) & \text{for } m = 0, 1, \cdots, N_s - 1 \\ 0 & \text{for } m = N_s, \cdots, N_{\text{IFFT}} - 1 \end{cases} \tag{46}$$

$$Y_2(b,m) = e^{\frac{\mathrm{j}2\pi bm}{N_{\text{IFFT}}}} \tag{47}$$

where $\mathrm{j} = \sqrt{-1}$. Thus (43) becomes

$$F_Z(z) \approx \int_{-\infty}^{z} \sum_{k=0}^{N_{\text{DFT}}-1} \left[\left(\sum_{m=0}^{N_{\text{IFFT}}-1} \left[Y_1(m) \times Y_2(b,m)\right] e^{\frac{\mathrm{j}2\pi am}{N_{\text{IFFT}}}}\right)^{N_{TX}}\right] dt \tag{48}$$

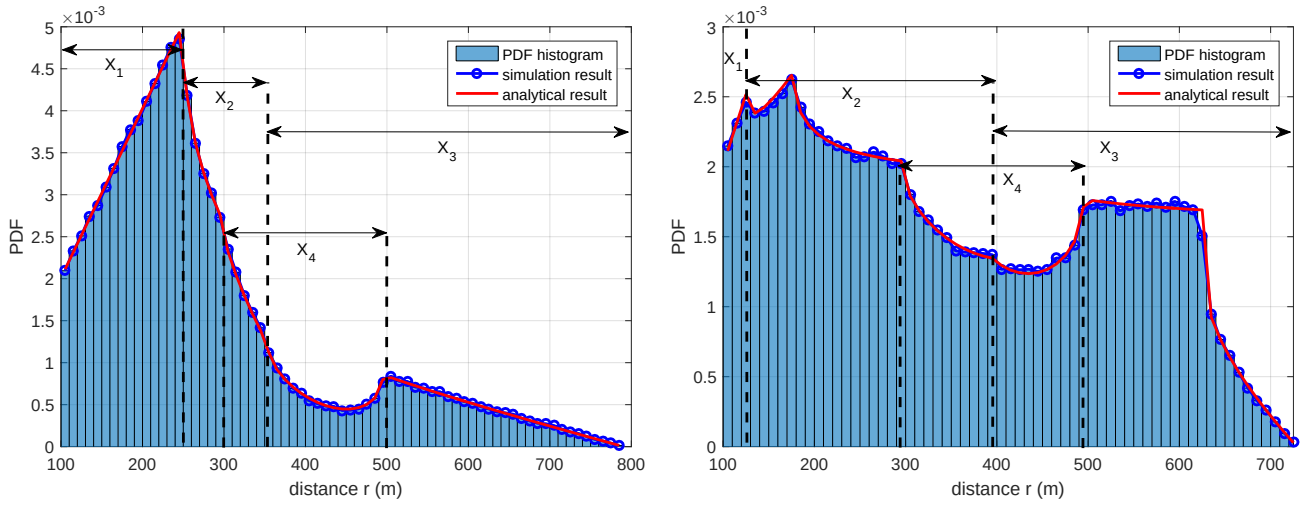

Fig. 6. PDF of the distance from a random GAA transmitter to PAL base stations of Fig. 2: (a) for PAL 1; (b) for PAL 2.

VI. Optimization of the Exclusion Zones

Given a certain exclusion zones' location and size, we can calculate the probability in (42). With the increase of the size of exclusion zones, the interference decreases, providing better interference protection for the PALs. However, GAA transmitters will be restricted to a smaller area within the census tract. To achieve a fair trade-off between the two networks, we seek an optimized exclusion zone pattern to meet the interference requirement as well as enlarge GAA transmitters area as much as possible. In other words, we want to find the smallest exclusion zone to keep the interference below the threshold.

A. Problem Formulation

The optimization problem is formulated as

$$\mathcal{P}: \begin{cases} \min & \sum_k \pi R_k^2 \\ \text{s.t.} & F_Z^j(I_0) > P_0 \\ \text{for} & 1 \le j \le N_{RX} \end{cases} \tag{49}$$

where $I_0 = -40dBm, P_0 = 0.99$ in the default case [4]. $F_Z^j(I_0)$ follows (42) and it is a function of $f_R(r)$ which is a function of R_k .

$F_Z^j(z)$ is a convex function of R_k if PAL receiver j is at the center of its own exclusion zone k. The convexity of $F_Z^j(z)$ of R_k is proved in Appendix A.

The convexity of $F_Z^j(z)$ in the domain of: 1) R_k of its own exclusion zone when PAL receiver j is not at the center of the exclusion zone and 2) R_k of other exclusion zones are difficult to prove. We define an exclusion zone as $\hat{k}$ with the radius $R_{\hat{k}}$ for those two cases. We propose to use a lower bound $f_R^-(r)$ for $f_R(r)$, given as (50) to tighten the constraint in (49).

where

$$h\left(R_{\hat{k}}\right) = -C_4(r) \times 2\arccos\left(\frac{r^2 + d_{j\hat{k}}^2 - w\left(R_{\hat{k}}\right)^2}{2d_{j\hat{k}}r}\right) \tag{51}$$

$$w\left(R_{\hat{k}}\right) = \left(R_{\hat{k}} - \left|r - d_{j\hat{k}}\right|\right)\frac{\sqrt{r^2 + d_{j\hat{k}}^2}}{r + d_{j\hat{k}}} + \left|r - d_{j\hat{k}}\right| \tag{52}$$

and $\max\left(\left|A_{\hat{k}}^e\right|\right) = \pi \max\left(R_{\hat{k}}\right)^2$. We consider the feasible range of $R_{\hat{k}}$ is finite according to the size of the census tract. $C_4(r) = r$, when $\frac{\partial D_k(r)}{\partial r}$ follows (26) and $\min\left(d_{jk}^X\right) < r < \max\left(d_{jk}^X\right)$; $C_4(r) = 2r$ for other cases.

We use $f_R^-(r)$ to replace $f_R(r)$ in the feasible range of r, $\left|d - R_{\hat{k}}\right| < r < \left|d + R_{\hat{k}}\right|$ to calculate $F_Z^j(z)$, defined as a lower bound $F_Z^{j-}(z)$. The convexity of $F_Z^{j-}(z)$ of $R_{\hat{k}}$ is proved in Appendix B.

The problem (49) is turned into a sub-optimal problem given as:

$$\mathcal{P}: \begin{cases} \min & \sum_k \pi R_k^2 \\ \text{s.t.} & F_Z^{j-}(I_0) > P_0 \\ \text{for} & 1 \le j \le N_{RX} \end{cases} \tag{53}$$

(53) can be numerically solved by using the MATLAB convex optimization tool and the optimization solver design is out of the scope of this paper.

VII. Numerical Results

To verify our analytical results, we build numerical simulations using the following parameters: The census tract area: $S_1 = 1000m, S_2 = 707.11m, S_3 = S_4 = 500m$, $V_1 = V_4 = \pi/2, V_2 = \pi/4, V_3 = 3\pi/4$. The transmit power of GAA base stations is $24dBm$ [4]. We place two PAL receivers in the census tract, the coordinates are $PAL_1 = \{250m, 250m\}$ and $PAL_2 = \{625m, 125m\}$ with V_1 as the reference point $\{0, 0\}$ as shown in Fig. 2.

$$f_R(r) > f_R^-(r) = \frac{2\pi r - \sum_l \frac{\partial B_l}{\partial r} + \sum_l \frac{\partial C_l}{\partial r} - \sum_{k=1,k\neq\hat{k}}^{N_E} \frac{\partial D_k}{\partial r} - \left(\frac{\partial D_{\hat{k}}}{\partial r} - C_4(r)\xi_{j\hat{k}}(r)\right)}{|A^c| - \sum_{k=1}^{N_E} \left|A_k^e\right|} + \frac{h\left(R_{\hat{k}}\right)}{|A^c| - \sum_{k=1,k\neq\hat{k}}^{N_E} \left|A_k^e\right| - \max\left(\left|A_{\hat{k}}^e\right|\right)} \quad (50)$$

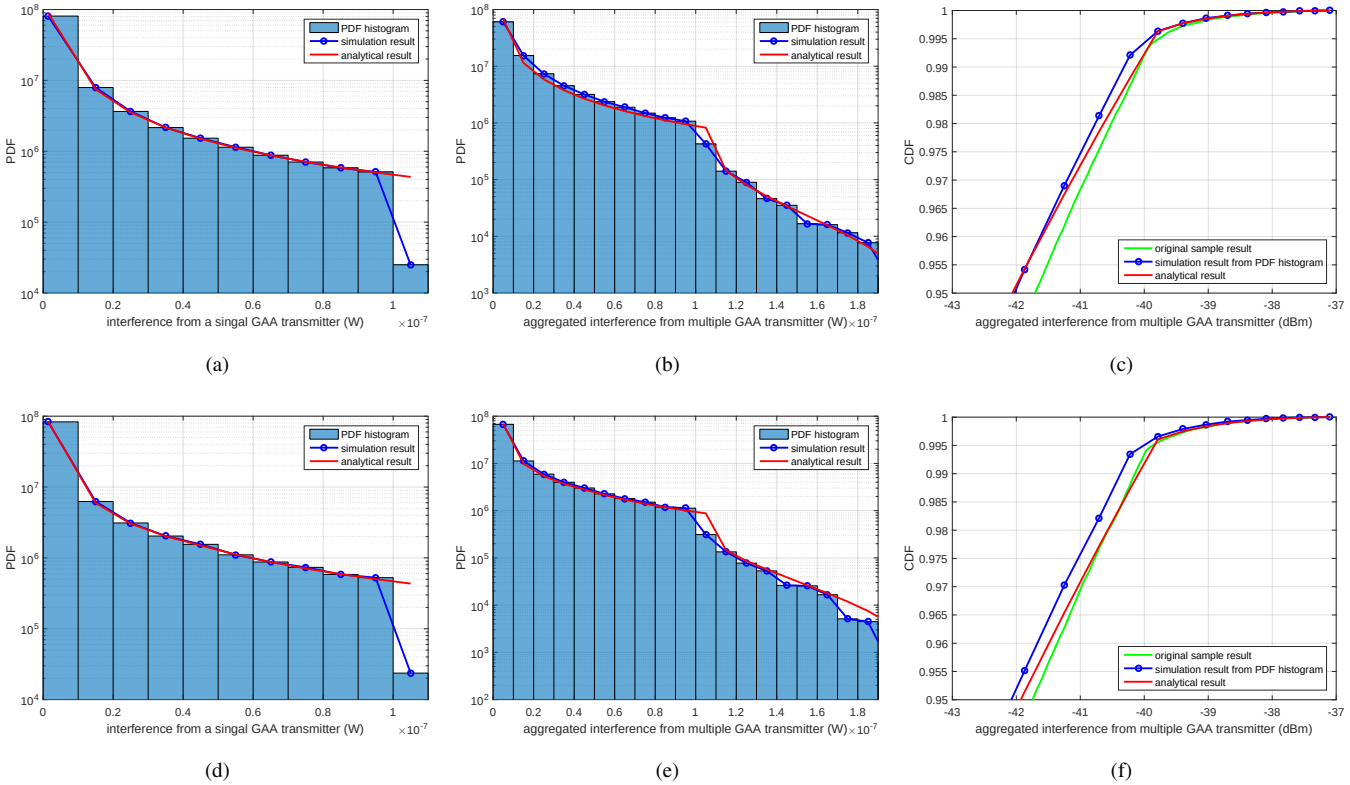

Fig. 7. Numerical results of the aggregated interference distribution: (a)-(c) are for PAL 1; (d)-(f) are for PAL 2.

Fig. 6 shows the PDF of the distance from GAA transmitters to PAL receivers. We indicated four sections in the ranges of r, illustrated as $X_1, ..., X_4$. These four ranges are determined by the intersection between circle $\{PAL_j, r\}, j = 1, 2$, the census tract boundary and the exclusion zones. For PAL 1 and 2 the sections are shown in Table. I and II respectively.

The intersection area variables in (6) and (28) are valid in different range of r as: 1) $B_l = 0, C_l = 0, D_k = 0, r \in X_1$; 2) $B_l > 0, C_l = 0, r \in X_2$; 3) $B_l > 0, C_l > 0, r \in X_3$ and 4) $D_l > 0, r \in X_4$.

TABLE I
SECTIONS OF THE DISTANCE FROM GAA TRANSMITTERS TO PAL 1

section	range	numerical value (m)
X_1	$R_1 < r \leq d_{S_1}$	$100 < r \leq 250$
X_2	$d_{S_1} < r \leq d_{V_1}$	$250 < r \leq 353.55$
X_3	$d_{V_1} < r < r_{max}$	$353.55 < r < 790.57$
X_4	$d_{PAL_2} - R_2 \geq r \leq d_{PAL_2} - R_2$	$295.28 < r \leq 495.28$

We use a LTE path loss model in [31], $L_{ij} = 43.3 \log_{10} d_{ij} + 11.5 + 20 \log_{10} f_c$. We choose the central frequency $f_c = 3.6$ GHz within the range 3.55 - 3.7 GHz. The feasible range of the radius of the exclusion zones of PAL 1 and 2 is $\{10m, 250m\}$, $\{10m, 125m\}$ respectively.

TABLE II
SECTIONS OF THE DISTANCE FROM GAA TRANSMITTERS TO PAL 2

section	range	numerical value (m)
X_1	$R_1 < r \leq d_{S_1}$	$100 < r \leq 125$
X_2	$d_{S_1} < r \leq d_{V_2}$	$125 < r \leq 395.28$
X_3	$d_{V_2} < r < r_{max}$	$395.28 < r < 728.87$
X_4	$d_{PAL_1} - R_2 \geq r \leq d_{PAL_1} - R_1$	$295.28 < r \leq 495.28$

The simulation and analytical results of the interference from one GAA transmitter to PAL receivers are shown in Fig. 7 (a) and (d) for PAL 1 and 2 respectively. We compare the simulation and analytical results for the aggregated interference when $N_{TX} = 2$ as shown in Fig. 7 (b) and (e). Moreover, the CDF of the aggregated interference results are shown in Fig. 7 (c) and (f). We focus on the CDF range close to 99%. We also put the original sample result which calculate $N_{TX} = 2$ random GAA aggregated interference using a Monte-Carlo simulation in comparison. Simulation and analytical results are integral of the PDF histogram data shown in Fig. 7 (b) and (e) respectively. The gap between the simulation results from PDF histogram and the original sample result is due to the MATLAB PDF histogram approximation. We can consider a certain margin in later design for this gap. From Fig. 6 and 7, we can see that the analytical results are close to the simulation

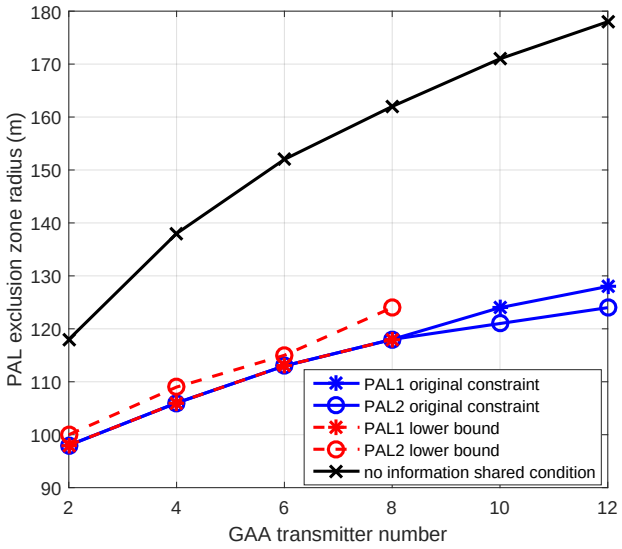

Fig. 8. Numerical results of optimization problem: Exclusion zone radius solution for optimization problem (49) and (53), with $I_0 = -40$ dBm and $P_0 = 0.99$.

results.

We present the solution for the optimization problem in (49) when $I_0 = -40$ dBm and $P_0 = 0.99$ in Fig. 8. The results show that with the increase of the GAA transmitter number, the PAL exclusion zone size increases as well. Moreover, with a small number of GAA transmitters, (i.e. $N_{TX} \leq 8$ in this scenario), the exclusion zone sizes of PAL 1 and PAL 2 are the same. However, with more GAA transmitters, i.e. $N_{TX} > 8$, PAL 1 needs a larger exclusion zone than PAL 2. As the location of PAL 1 is more central, there is a higher probability of PAL 1 suffering from interference. When the number of GAAs increases, this effect is more prominent, hence requiring a larger radius than PAL 2. We also show the sub-optimal approach in (53) in Fig. 8 for comparison. We assume that the exclusion zones do not exceed the census tract boundary and maximum exclusion zone radius for PAL 1 and PAL 2 is 250m and 125m respectively. For the same GAA transmitter number, the sub-optimal approach in (53) requires a larger exclusion zone size than the original problem in (49). In Fig. 8, we can see the increase in PAL 2 exclusion zone. Since in the lower bound equation (50) we use PAL 1 maximum exclusion zone size for PAL 2 constraint, PAL 1 maximum exclusion zone has a larger difference with the exclusion zone size range in the solution.

Moreover, we compare our results with the exclusion zones when there is no information shared between two SASs. We focus on one PAL and assume that the distribution of the base stations of the other SAS is unknown. For a certain number of possible transmitters N_{TX}, the maximum interference occurs when all the GAA transmitters have the same distance to a PAL receiver. Thus the exclusion zone size which can guarantee that the aggregated interference is below -40 dBm can be calculated as:

$$R_k = d_0 \left(\frac{P_t N_{TX} K}{I_0} \right)^{1/\beta} \tag{54}$$

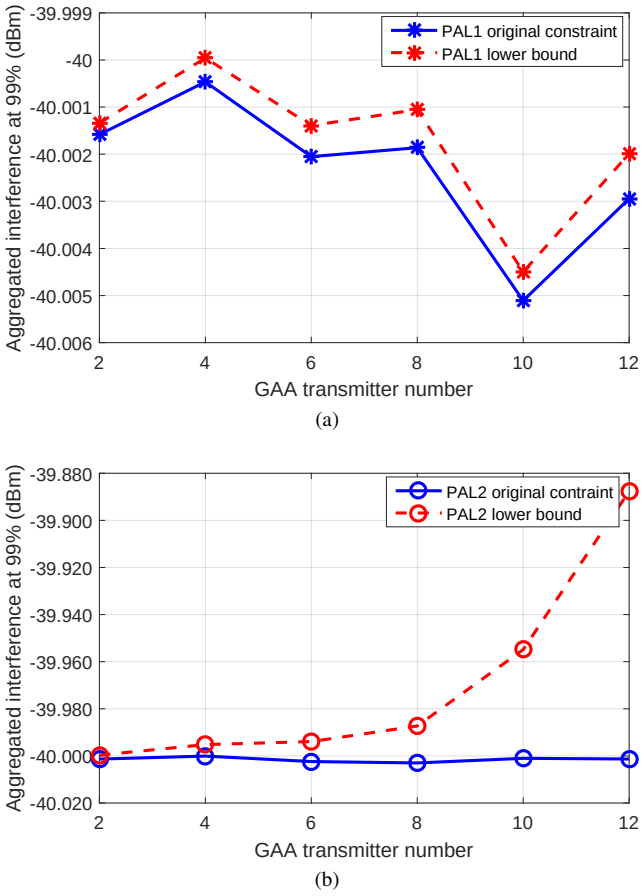

Fig. 9. Difference between the results using the original constraint and the lower bound. Aggregated interference for PAL 1 and 2 is shown in (a) and (b) respectively when the input probability for the CDF of aggregated interference is 0.99 and at the same time the optimum exclusion zone size solution of (49), as shown in Fig. 8 labeled with original constraints.

The result of (54) when no information is shared is also shown in Fig. 8 for comparison. With the same number of GAA transmitters, our method shrinks the exclusion zone size by 16.96%-27.16% that provides GAA network more opportunities to transmit. Note that PAL knowing all GAA locations is a less comparable scenario, as it results in a combinatorial problem to pick the GAA users that can transmit. Exclusion zones cannot be defined in this scenario. Furthermore, to show the difference between the optimum and sub-optimal solutions, we calculate the aggregated interference level when: 1) the input probability for the CDF of aggregated interference is 99% and at the same time 2) the optimum exclusion zone size solution of (49), as shown in Fig. 8 labeled with original constraints. For PAL 1, the results are shown in Fig. 9 (a). We can see that the sub-optimal constraints will cause more interference, however, the interference level is still below -40 dBm and the gap is very narrow, approximately 0.001 dB. For PAL 2, the results are shown in Fig. 9 (b). We can see that the sub-optimal constraints will cause more interference, the interference level is above -40 dBm and the gap is approximately -0.12 dB. With the optimum exclusion zone size, PAL 2 can not meet the interference requirements using the sub-optimal constraints. Since the sub-optimal solutions

are obtained with a lower bound of the constraints, they will generate more interference with the same exclusion zone size. These results coincide with our analytical results. The gaps between the optimum and sub-optimal solutions are narrow that we can use the sub-optimal solutions as network design references.

VIII. Conclusion

In this paper, we proposed a method for inter-operator interference mitigation in Spectrum Access System between Priority Access and General Authorized Access base stations. Our method does not require or expose the exact locations of any base stations. GAA base stations share their location distribution and the number of transmitters in a closed finite census tract area and the PAL network can derive and calculate the distribution of aggregated interference from the GAA base stations. Furthermore, we consider the practical implementation with the Inverse Fast Fourier Transform and Discrete Fourier Transform. Moreover, we proposed a novel way of using the exclusion zone to protect PAL base stations. According to the distribution of aggregated interference, the PAL network can design and optimize its exclusion zone. We proposed a convex lower bound to approximate the non-convex optimization problem. Simulation results show that the lower bound provides a good approximation. Our approach reduces the exclusion zone size by over 16%, which gives significantly more spectral opportunities to GAA in the spatial domain. Our method meets the interference requirements of SAS, keeps the fairness between PAL and GAA networks and protects the location information of both networks.

Appendix A
Convexity of $F_Z^j(z)$ of R_k

According to (41),

$$\frac{\partial^2 F_Z^j(z)}{\partial R_k^2} = \int_{-\infty}^{z} \frac{\partial^2 f_Z(t)}{\partial R_k^2} dt \tag{55}$$

Define $g(y) = \underbrace{f_Y(y) * f_Y(y) * ... * f_Y(y)}_{N_{TX}-1}$

$$\frac{\partial^2 f_Z(t)}{\partial R_k^2} = \frac{\partial^2 (f_Y(y) * g(y))}{\partial R_k^2} = \frac{\partial^2 f_Y(y)}{\partial R_k^2} * g(y) \tag{56}$$

where

$$\frac{\partial^2 f_Y(y)}{\partial R_k^2} = \left|\frac{dr}{dy}\right| \times \frac{\partial^2 f_R(r)}{\partial R_k^2} \tag{57}$$

$$\frac{\partial^2 f_R(r)}{\partial R_k^2} = C(r) \frac{\partial^2 g(R_k)}{\partial R_k^2} \tag{58}$$

where $C(r) = 2\pi r - \sum_l \frac{\partial B_l}{\partial r} + \sum_l \frac{\partial C_l}{\partial r} - \sum_{k=1}^{N_E} \frac{\partial D_k}{\partial r} > 0$ is a function of r only.

Define

$$g(R_k) = \frac{1}{|A^c| - \sum_{n=1}^{N_E} |A_n^e|} = \frac{1}{C - \pi R_k^2} \tag{59}$$

where $C = |A^c| - \sum_{n=1, n\neq k}^{N_E} |A_n^e|$ is constant with the change of R_k.

$$\frac{\partial^2 g(R_k)}{\partial R_k^2} = \frac{2\pi \left(C - \pi R_k^2 + 4\pi R_k\right)}{(C - \pi R_k^2)^3} \tag{60}$$

$\frac{\partial^2 g(R_k)}{\partial R_k^2} > 0$, $\frac{\partial^2 f_R(r)}{\partial R_k^2} > 0$, $\frac{\partial^2 f_Y(y)}{\partial R_k^2} > 0$ and $\frac{\partial^2 F_Z(z)}{\partial R_k^2} > 0$. Thus $F_Z(z)$ is convex of R_k.

Appendix B
Convexity of $F_Z^{j^-}(z)$ of $R_{\hat{k}}$

$$\begin{aligned}
f_R(r) &= \frac{2\pi r - \sum_l \frac{\partial B_l}{\partial r} + \sum_l \frac{\partial C_l}{\partial r} - \sum_{k=1, k\neq\hat{k}}^{N_E} \frac{\partial D_k}{\partial r} - \frac{\partial D_{\hat{k}}}{\partial r}}{|A^c| - \sum_{k=1}^{N_{RX}} \left|A_k^e\right|} \\
&= \frac{2\pi r - \sum_l \frac{\partial B_l}{\partial r} + \sum_l \frac{\partial C_l}{\partial r} - \sum_{k=1, k\neq\hat{k}}^{N_E} \frac{\partial D_k}{\partial r}}{|A^c| - \sum_{k=1}^{N_E} \left|A_k^e\right|} \\
&+ \frac{-\left(C_4(r)\xi_{j\hat{k}}(r) + C_5(r)\right)}{|A^c| - \sum_{k=1}^{N_E} \left|A_k^e\right|} \\
&> \frac{2\pi r - \sum_l \frac{\partial B_l}{\partial r} + \sum_l \frac{\partial C_l}{\partial r} - \sum_{jk=1, k\neq\hat{k}}^{N_E} \frac{\partial D_k}{\partial r} - C_5(r)}{|A^c| - \sum_{k=1, k\neq\hat{k}}^{N_E} \left|A_k^e\right| - \left|A_{\hat{k}}^e\right|} \\
&+ \frac{-C_4(r)\xi_{j\hat{k}}(r)}{|A^c| - \sum_{k=1, k\neq\hat{k}}^{N_E} \left|A_k^e\right| - \max\left(\left|A_{\hat{k}}^e\right|\right)} \\
&= \frac{C_1(r)}{C_2 - \pi R_{\hat{k}}^2} + \frac{-C_4(r)\xi_{j\hat{k}}(r)}{C_3} > \frac{C_1(r)}{C_2 - \pi R_{\hat{k}}^2} + \frac{h\left(R_{\hat{k}}\right)}{C_3}
\end{aligned} \tag{61}$$

where $C_1(r)$, C_2, C_3, $C_4(r)$ and $C_5(r)$ are positive constants with the change of $R_{\hat{k}}$. $C_5(r) = \frac{\partial D_{\hat{k}}}{\partial r} - C_4(r)\xi_{j\hat{k}}(r)$. $\frac{C_1(r)}{C_2 - \pi R_{\hat{k}}^2}$ is convex, the proof follows the same process as Appendix A.

We focus on $-C_4(r)\xi_{j\hat{k}}(r)$ and we propose a lower bound as:

$$h\left(R_{\hat{k}}\right) = -C_4(r) \times 2 \arccos\left(\frac{r^2 + d_{j\hat{k}}^2 - w\left(R_{\hat{k}}\right)^2}{2 d_{j\hat{k}} r}\right) \tag{62}$$

$C_4(r)$ follows (31) and (26) depends on different exclusion zone settings,

$$w\left(R_{\hat{k}}\right) = \left(R_{\hat{k}} - \left|r - d_{j\hat{k}}\right|\right) \frac{\sqrt{r^2 + d_{j\hat{k}}^2}}{r + d_{j\hat{k}}} + \left|r - d_{j\hat{k}}\right| < R_{\hat{k}} \tag{63}$$

For $\left|r - d_{j\hat{k}}\right| \leq R_{\hat{k}} \leq \sqrt{r^2 + d_{j\hat{k}}^2}$, $-C_4(r)\xi_{j\hat{k}}(r)$ is convex. However, for $\sqrt{r^2 + d_{j\hat{k}}^2} \leq R_{\hat{k}} \leq r + d_{j\hat{k}}$, $-C_4(r)\xi_{j\hat{k}}(r)$ is concave. Thus we design a convex lower bound $h\left(R_{\hat{k}}\right)$ for $-C_4(r)\xi_{j\hat{k}}(r)$ by stretching the convex part. The lower bound proof is given as:

$$\begin{aligned}
&h\left(R_{\hat{k}}\right) - \left(-C_4(r)\xi_{j\hat{k}}(r)\right) = -C_4(r) \times \\
&\left(2 \arccos\left(\frac{r^2 + d_{j\hat{k}}^2 - w\left(R_{\hat{k}}\right)^2}{2 d_{j\hat{k}} r}\right) - \xi_{j\hat{k}}(r)\right)
\end{aligned} \tag{64}$$

Since the cosine function is decreasing in $\{0, \pi\}$, we turn the proof into:

$$2\left(\frac{r^2+d_{j\hat{k}}^2-w\left(R_{\hat{k}}\right)^2}{2d_{j\hat{k}}r}\right)^2-1-\left(\frac{r^2+d_{j\hat{k}}^2-R_{\hat{k}}^2}{2d_{j\hat{k}}r}\right)$$
$$<2\left(\frac{r^2+d_{j\hat{k}}^2-w\left(R_{\hat{k}}\right)^2}{2d_{j\hat{k}}r}\right)^2-1-\left(\frac{r^2+d_{j\hat{k}}^2-w\left(R_{\hat{k}}\right)^2}{2d_{j\hat{k}}r}\right)$$
$$=\left(\frac{r^2+d_{j\hat{k}}^2-w\left(R_{\hat{k}}\right)^2}{d_{j\hat{k}}r}+1\right)\left(\frac{r^2+d_{j\hat{k}}^2-w\left(R_{\hat{k}}\right)^2}{2d_{j\hat{k}}r}-1\right) \quad (65)$$

Since $\left|r-d_{j\hat{k}}\right| \le w\left(R_{\hat{k}}\right) \le \sqrt{r^2+d_{j\hat{k}}^2}$, (65) < 0,

$$2\left(\frac{r^2+d_{j\hat{k}}^2-w\left(R_{\hat{k}}\right)^2}{2d_{j\hat{k}}r}\right)^2-1<\frac{r^2+d_{j\hat{k}}^2-R_{\hat{k}}^2}{2d_{j\hat{k}}r} \quad (66)$$

$$2\left(\cos\left(\arccos\left(\frac{r^2+d_{j\hat{k}}^2-w\left(R_{\hat{k}}\right)^2}{2d_{j\hat{k}}r}\right)\right)\right)^2-1<\cos\left(\xi_{j\hat{k}}(r)\right) \quad (67)$$

$$\cos\left(2\arccos\left(\frac{r^2+d_{j\hat{k}}^2-w\left(R_{\hat{k}}\right)^2}{2d_{j\hat{k}}r}\right)\right)<\cos\left(\xi_{j\hat{k}}(r)\right) \quad (68)$$

$$2\arccos\left(\frac{r^2+d_{j\hat{k}}^2-w\left(R_{\hat{k}}\right)^2}{2d_{j\hat{k}}r}\right)>\xi_{j\hat{k}}(r) \quad (69)$$

Thus (64) < 0, $h\left(R_{\hat{k}}\right) < -C_4(r)\xi_{j\hat{k}}(r)$ is a lower bound. Since $\left|r-d_{j\hat{k}}\right| \le w\left(R_{\hat{k}}\right) \le \sqrt{r^2+d_{j\hat{k}}^2}$, $h\left(R_{\hat{k}}\right)$ is convex. Our lower bound of $f_R(r)$ is

$$f_R^-(r)=\frac{C_1(r)}{C_2-\pi R_{\hat{k}}^2}+\frac{h\left(R_{\hat{k}}\right)}{C_3}<f_R(r) \quad (70)$$

is convex, thus $F_Z^{j-}(z)$ is a convex function of $R_{\hat{k}}$.

Acknowledgment

Ying He is a recipient of an International Research Scholarship and a Faculty of Engineering and Information Technology Scholarship, University of Technology Sydney. This work has been supported in part by Intel's University Research Office.

References

[1] J. G. Andrews, S. Buzzi, W. Choi, S. V. Hanly, A. Lozano, A. C. K. Soong, and J. C. Zhang, "What will 5G be?" *IEEE Journal on Selected Areas in Communications*, vol. 32, no. 6, pp. 1065–1082, June 2014.

[2] A. Osseiran, F. Boccardi, V. Braun, K. Kusume, P. Marsch, M. Maternia, O. Queseth, M. Schellmann, H. Schotten, H. Taoka, H. Tullberg, M. A. Uusitalo, B. Timus, and M. Fallgren, "Scenarios for 5G mobile and wireless communications: the vision of the METIS project," *IEEE Communications Magazine*, vol. 52, no. 5, pp. 26–35, May 2014.

[3] *System requirements for operation of Mobile Broadband Systems in the 2300 MHz - 2400 MHz band under Licensed Shared Access (LSA)*, ETSI Reconfigurable Radio Systems (RRS) Std. ETSI TS 103 154 V1.1.1, Tech. Rep., Oct. 2014.

[4] *Amendment of the Commission Rules with Regard to Commercial Operations in the 3550-3650 MHz Band*, Federal Communications Commission Std. GN Docket No. 12-354, Tech. Rep., Apr. 2015.

[5] *Amendment of the Commission Rules with Regard to Commercial Operations in the 3550-3650 MHz Band*, Federal Communications Commission Std. FCC 16-55 A1,GN Docket No. 12-354, Tech. Rep., May 2016.

[6] M. D. Mueck, S. Srikanteswara, and B. Badic, "Spectrum sharing: Licensed shared access (LSA) and spectrum access system (SAS)," October 2015. [Online]. Available: www.intel.com/content/dam/www/public/us/en/documents/white-papers/spectrum-sharing-lsa-sas-paper.pdf

[7] M. M. Sohul, M. Yao, T. Yang, and J. H. Reed, "Spectrum access system for the citizen broadband radio service," *IEEE Communications Magazine*, vol. 53, no. 7, pp. 18–25, July 2015.

[8] "SAS to CBSD protocol technical Report-B," *WInnF Spectrum Sharing Committee (SSC) of the Wireless Innovation Forum (WInnF)*, no. WINNF-15-P-0062-1.0.0, March 2016.

[9] "Requirements for commercial operation in the U.S. 3550-3700 MHz citizens broadband radio service band," *WInnF Spectrum Sharing Committee (SSC) of the Wireless Innovation Forum (WInnF)*, no. WINNF-15-S-0112-1.0.0, May 2016.

[10] "Interim SAS to SAS protocol technical Report-A," *WInnF Spectrum Sharing Committee (SSC) of the Wireless Innovation Forum (WInnF)*, no. WINNF-15-P-0051-1.0.0, January 2015.

[11] "Interim SAS to SAS protocol technical Report-B," *WInnF Spectrum Sharing Committee (SSC) of the Wireless Innovation Forum (WInnF)*, no. WINNF-16-P-0003-1.0.0, April 2016.

[12] B. Jayawickrama, E. Dutkiewicz, M. Mueck, and Y. He, "On the usage of geolocation aware spectrum measurements for incumbent location and transmit power detection," *IEEE Transactions on Vehicular Technology*, to be published.

[13] L. Vijayandran, P. Dharmawansa, T. Ekman, and C. Tellambura, "Analysis of aggregate interference and primary system performance in finite area cognitive radio networks," *IEEE Transactions on Communications*, vol. 60, no. 7, pp. 1811–1822, July 2012.

[14] C. h. Lee and M. Haenggi, "Interference and outage in poisson cognitive networks," *IEEE Transactions on Wireless Communications*, vol. 11, no. 4, pp. 1392–1401, April 2012.

[15] S. Kusaladharma, P. Herath, and C. Tellambura, "Underlay interference analysis of power control and receiver association schemes," *IEEE Transactions on Vehicular Technology*, to be published.

[16] A. Shojaeifard, K. A. Hamdi, E. Alsusa, D. K. C. So, and J. Tang, "Exact SINR statistics in the presence of heterogeneous interferers," *IEEE Transactions on Information Theory*, vol. 61, no. 12, pp. 6759–6773, Dec 2015.

[17] J. Guo, S. Durrani, and X. Zhou, "Outage probability in arbitrarily-shaped finite wireless networks," *IEEE Transactions on Communications*, vol. 62, no. 2, pp. 699–712, February 2014.

[18] J. Guo, S. Durrani, and X. Zhou, "Performance analysis of arbitrarily-shaped underlay cognitive networks: Effects of secondary user activity protocols," *IEEE Transactions on Communications*, vol. 63, no. 2, pp. 376–389, Feb 2015.

[19] Z. Khalid and S. Durrani, "Distance distributions in regular polygons," *IEEE Transactions on Vehicular Technology*, vol. 62, no. 5, pp. 2363–2368, Jun 2013.

[20] E. Drocella, J. Richards, R. Sole, F. Najmy, A. Lundy, and P. McKenna, "3.5 Ghz exclusion zone analyses and methodology," June 2015. [Online]. Available: www.its.bldrdoc.gov/publications/download/TR-15-517r1.pdf

[21] C. W. Kim, J. Ryoo, and M. M. Buddhikot, "Design and implementation of an end-to-end architecture for 3.5 Ghz shared spectrum," in *Dynamic Spectrum Access Networks (DySPAN), 2015 IEEE International Symposium on*, Sept 2015, pp. 23–34.

[22] J. Ojaniemi, J. H. Poikonen, and R. Wichman, "Optimization of secondary system antenna deployment in shared spectrum access," *IEEE Transactions on Vehicular Technology*, vol. 65, no. 5, pp. 3536–3546, May 2016.

[23] U. Tefek and T. J. Lim, "Interference management through exclusion zones in two-tier cognitive networks," *IEEE Transactions on Wireless Communications*, vol. 15, no. 3, pp. 2292–2302, March 2016.

[24] A. Ullah, S. Bhattarai, J. M. Park, J. H. Reed, D. Gurney, and B. Bahrak, "Multi-tier exclusion zones for dynamic spectrum sharing," in *2015 IEEE International Conference on Communications (ICC)*, June 2015, pp. 7659–7664.

[25] S. Bhattarai, A. Ullah, J. M. J. Park, J. H. Reed, D. Gurney, and B. Gao, "Defining incumbent protection zones on the fly: Dynamic boundaries

for spectrum sharing," in *Dynamic Spectrum Access Networks (DySPAN), 2015 IEEE International Symposium on*, Sept 2015, pp. 251–262.
[26] A. Goldsmith, *Wireless communications*. Cambridge university press, 2005.
[27] H. Tanizaki, *Computational methods in statistics and econometrics*. CRC Press, 2004.
[28] A. Rényi, *Foundations of Probability*. Courier Corporation, 2007.
[29] V. Skorokhod, *Basic principles and applications of probability theory*. Springer Science & Business Media, 2005.
[30] Y. He, J. Wang, Y. Su, E. Dutkiewicz, X. Huang, and J. Shi, "An efficient implementation of PRACH generator in LTE UE transmitters," in *Wireless Communications and Mobile Computing Conference (IWCMC), 2011 7th International*, July 2011, pp. 2226–2230.
[31] *3rd Generation Partnership Project; Technical Specification Group Radio Access Network; Evolved Universal Terrestrial Radio Access (E-UTRA); Further advancements for E-UTRA physical layer aspects (Release 9)*, 3GPP Std. Tech. Spec. 36.814 v9.0.0, Mar. 2010.